Modeling and Analysis of Three-phase Inverter based on Generalized State Space Averaging Method

Zhao Lin, Hao Ma
College of Electrical Engineering, Zhejiang University, Hangzhou, China, 310027
E-mail: mahao@cee.zju.edu.cn

***Abstract*—Aiming at the deficiency of common methods in inverter modeling, the modeling of three-phase three-wire inverter based on generalized state space averaging method is presented in this paper, which also takes the dead-time effect into consideration. By using the proposed method, the calculating fundamental components of voltages and currents are in accord with the simulation and experiment of actual devices considerably compared with conventional state-space averaging method. Besides, it provides effective means for precise closeloop controller design. The simulations by means of Matlab are well developed to describe the proposed theoretical model. In addition, an experimental platform based on three-phase three-wire inverters is built and shown to validate the effectiveness of the mathematical results.**

Keywords—Generalized state space averaging; three-phase three-wire inverter; dead-time effect; modeling; simulation and experiment.

I. INTRODUCTION

When studying the inverters and their dynamic performance, precise switching models are established based on the switching of switch state, which is feasible for a single inverter or small-scale inverter system. However, switching models for middle-scale or large-scale inverter systems are complicated [1]-[2]. State-space averaging method is also shown to be an effective method for analysis and controller design in inverters [3]-[5]. However, it is difficult to guarantee high accuracy of steady-state and large-signal dynamic process.

Different from accurate switching model and state-space averaging method, generalized state space averaging model considers the average of the state variables as well as the harmonics [6], and facilitates the calculation of fundamental components of voltages and currents with a desired precision. Besides, it conveniences the analysis of steady-state and transient process. Although conventional switching models and state-space averaging methods which take dead-time effects into consideration have been applied successfully in the inverters [7]-[8], the modeling of three-phase inverter with dead-time effects based on generalized state space averaging method has not been investigated so far.

The basic principle of the generalized averaging technique is introduced in Section II. Modeling of three-phase three-wire inverter with dead-time effect based on generalized averaging method is presented in Section III. In order to verify the correctness of the mathematical model, simulation and experimental data and curves are shown in Section IV. Finally, the conclusion is proposed in Section V.

II. GENERALIZED STATE SPACE AVERAGING METHOD

Generalized state space averaging method is based on Fourier transform. If time-domain periodic signal *x(t)* satisfies the following condition $\int_0^T |x(t)|^2\, dt < \infty$, it can be approximated on the interval [t-T, t] to arbitrary accuracy with a Fourier series representation of the form

$$x(t) = \sum_{k=-\infty}^{\infty} \langle x \rangle_k (t) e^{jk\omega t} \tag{1}$$

where, $\omega=2\pi/T$ is fundamental angular frequency, and $\langle x \rangle_k (t)$ are the k th Fourier coefficients, which are determined by

$$\langle x \rangle_k (t) = \frac{1}{T}\int_{t-T}^{t} x(\tau) e^{-jk\omega\tau} d\tau \tag{2}$$

If *x(t)* is real signal, it has

$$\langle x \rangle_k = \langle x \rangle_k^{\mathrm{Re}} + j\langle x \rangle_k^{\mathrm{Im}} = \langle x \rangle_{-k}^{*} = \langle x \rangle_{-k}^{\mathrm{Re}} - j\langle x \rangle_{-k}^{\mathrm{Im}} \tag{3}$$

Two important characteristics of Fourier transform will be utilized in the modeling of inverter in the next section, which are expressed by

$$\frac{d}{dt}\langle x \rangle_k (t) = \left\langle \frac{d}{dt} x \right\rangle_k (t) - jk\omega \langle x \rangle_k (t) \tag{4}$$

$$\langle xy \rangle_k = \sum_{i=-\infty}^{\infty} \langle x \rangle_{k-i} \langle y \rangle_i \tag{5}$$

III. MODELING OF INVERTER WITH DEAD-TIME EFFECT

The circuit of three-phase three-wire voltage source inverter is shown in Fig.1.

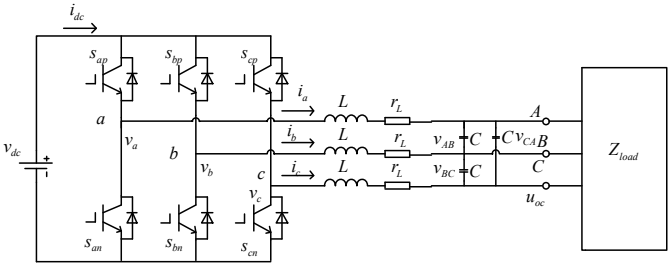

Fig. 1. Three-phase three-wire voltage source inverter

The switching function is defined by

$$s_{ik}=\begin{cases}1 & \text{switch is closed}\\ 0 & \text{switch is opened}\end{cases} \tag{6}$$

where, $i\in\{a,b,c\}$, $k\in\{p,n\}$, $s_{ip}+s_{in}=1$.

Especially, the following relationship is not hard to be attained

$$s_i=s_{ip}=1-s_{in} \tag{7}$$

Assuming that the loads are three-phase symmetrical resistive loads in delta connection, whose value are R, we obtain

$$\begin{bmatrix}v_{ab}\\ v_{bc}\\ v_{ca}\end{bmatrix}=\begin{bmatrix}v_a-v_b\\ v_b-v_c\\ v_c-v_a\end{bmatrix}=L\frac{d}{dt}\begin{bmatrix}i_a-i_b\\ i_b-i_c\\ i_c-i_a\end{bmatrix}+r_L\begin{bmatrix}i_a-i_b\\ i_b-i_c\\ i_c-i_a\end{bmatrix}+\begin{bmatrix}v_{AB}\\ v_{BC}\\ v_{CA}\end{bmatrix} \tag{8}$$

$$\begin{bmatrix}i_{ab}\\ i_{bc}\\ i_{ca}\end{bmatrix}=C\frac{d}{dt}\begin{bmatrix}v_{AB}\\ v_{BC}\\ v_{CA}\end{bmatrix}+\frac{1}{R}\begin{bmatrix}v_{AB}\\ v_{BC}\\ v_{CA}\end{bmatrix} \tag{9}$$

where, i_{ab}, i_{bc}, i_{ca} are virtual line currents, which are calculated by

$$i_a=i_{ab}-i_{ca}\,,i_b=i_{bc}-i_{ab}\,,i_c=i_{ca}-i_{bc}$$

$$i_{ab}=\frac{1}{3}(i_a-i_b)\,,i_{bc}=\frac{1}{3}(i_b-i_c)\,,i_{ca}=\frac{1}{3}(i_c-i_a) \tag{10}$$

The following equation is not difficult to be built

$$\begin{bmatrix}v_{ab}\\ v_{bc}\\ v_{ca}\end{bmatrix}=\begin{bmatrix}v_a-v_b\\ v_b-v_c\\ v_c-v_a\end{bmatrix}=\begin{bmatrix}s_a-s_b\\ s_b-s_c\\ s_c-s_a\end{bmatrix}\bullet v_{dc} \tag{11}$$

Thus, the conventional state equations of three-phase inverter are easily to be constructed

$$\begin{cases}\dfrac{d}{dt}\begin{bmatrix}i_{ab}\\ i_{bc}\\ i_{ca}\end{bmatrix}=-\dfrac{r_L}{L}\begin{bmatrix}i_{ab}\\ i_{bc}\\ i_{ca}\end{bmatrix}-\dfrac{1}{3L}\begin{bmatrix}v_{AB}\\ v_{BC}\\ v_{CA}\end{bmatrix}+\dfrac{1}{3L}\begin{bmatrix}s_a-s_b\\ s_b-s_c\\ s_c-s_a\end{bmatrix}\bullet v_{dc}\\ \dfrac{d}{dt}\begin{bmatrix}v_{AB}\\ v_{BC}\\ v_{CA}\end{bmatrix}=-\dfrac{1}{RC}\begin{bmatrix}v_{AB}\\ v_{BC}\\ v_{CA}\end{bmatrix}+\dfrac{1}{C}\begin{bmatrix}i_{ab}\\ i_{bc}\\ i_{ca}\end{bmatrix}\end{cases} \tag{12}$$

where L is filtering inductor, C is filtering capacitor, r_L is the ESR of inductor, i_{ab}, i_{bc}, i_{ca}, v_{AB}, v_{BC}, v_{CA} are the state variables.

If we use the SPWM technique, s_k can be replaced by its fundamental component d_k

$$d_k=\frac{1}{2}(1+\frac{v_m}{V_{tri}})=\frac{m}{2}\cos(\omega t-\varphi_k)+\frac{1}{2} \tag{13}$$

where, $k=a,b,c$, $\varphi_a=\varphi_0$, $\varphi_b=\varphi_0+2\pi/3$, $\varphi_c=\varphi_0-2\pi/3$, φ_0 is initial phase angle, m is amplitude modulation ratio.

Combined by equation (13), equation (12) is rewritten as

$$\begin{cases}\dfrac{d}{dt}\begin{bmatrix}i_{ab}\\ i_{bc}\\ i_{ca}\end{bmatrix}=-\dfrac{r_L}{L}\begin{bmatrix}i_{ab}\\ i_{bc}\\ i_{ca}\end{bmatrix}-\dfrac{1}{3L}\begin{bmatrix}v_{AB}\\ v_{BC}\\ v_{CA}\end{bmatrix}+\dfrac{\sqrt{3}m}{6L}\begin{bmatrix}v_{dc}\cos(\omega t-\varphi_a+\dfrac{\pi}{6})\\ v_{dc}\cos(\omega t-\varphi_b+\dfrac{\pi}{6})\\ v_{dc}\cos(\omega t-\varphi_c+\dfrac{\pi}{6})\end{bmatrix}\\ \dfrac{d}{dt}\begin{bmatrix}v_{AB}\\ v_{BC}\\ v_{CA}\end{bmatrix}=-\dfrac{1}{RC}\begin{bmatrix}v_{AB}\\ v_{BC}\\ v_{CA}\end{bmatrix}+\dfrac{1}{C}\begin{bmatrix}i_{ab}\\ i_{bc}\\ i_{ca}\end{bmatrix}\end{cases} \tag{14}$$

The state variables of the above equation can be approximated to the sum of their DC components and fundamental components

$$\begin{cases}i_{ab}\approx\langle i_{ab}\rangle_{-1}e^{-j\omega t}+\langle i_{ab}\rangle_0+\langle i_{ab}\rangle_1 e^{j\omega t}\\ i_{bc}\approx\langle i_{bc}\rangle_{-1}e^{-j\omega t}+\langle i_{bc}\rangle_0+\langle i_{bc}\rangle_1 e^{j\omega t}\\ i_{ca}\approx\langle i_{ca}\rangle_{-1}e^{-j\omega t}+\langle i_{ca}\rangle_0+\langle i_{ca}\rangle_1 e^{j\omega t}\\ v_{AB}\approx\langle v_{AB}\rangle_{-1}e^{-j\omega t}+\langle v_{AB}\rangle_0+\langle v_{AB}\rangle_1 e^{j\omega t}\\ v_{BC}\approx\langle v_{BC}\rangle_{-1}e^{-j\omega t}+\langle v_{BC}\rangle_0+\langle v_{BC}\rangle_1 e^{j\omega t}\\ v_{CA}\approx\langle v_{CA}\rangle_{-1}e^{-j\omega t}+\langle v_{CA}\rangle_0+\langle v_{CA}\rangle_1 e^{j\omega t}\end{cases} \tag{15}$$

Combining equations (4), (14) and (15), generalized state space averaging model of three-phase three-wire inverter can be expressed by

$$\begin{cases}\dfrac{d}{dt}\begin{bmatrix}\langle i_{ab}\rangle_1\\ \langle i_{bc}\rangle_1\\ \langle i_{ca}\rangle_1\end{bmatrix}=-\dfrac{r_L}{L}\begin{bmatrix}\langle i_{ab}\rangle_1\\ \langle i_{bc}\rangle_1\\ \langle i_{ca}\rangle_1\end{bmatrix}-\dfrac{1}{3L}\begin{bmatrix}\langle v_{AB}\rangle_1\\ \langle v_{BC}\rangle_1\\ \langle v_{CA}\rangle_1\end{bmatrix}+\dfrac{\sqrt{3}m}{6L}\begin{bmatrix}\left\langle v_{dc}\cos(\omega t-\varphi_a+\dfrac{\pi}{6})\right\rangle_1\\ \left\langle v_{dc}\cos(\omega t-\varphi_b+\dfrac{\pi}{6})\right\rangle_1\\ \left\langle v_{dc}\cos(\omega t-\varphi_c+\dfrac{\pi}{6})\right\rangle_1\end{bmatrix}-j\omega\begin{bmatrix}\langle i_{ab}\rangle_1\\ \langle i_{bc}\rangle_1\\ \langle i_{ca}\rangle_1\end{bmatrix}\\ \dfrac{d}{dt}\begin{bmatrix}\langle v_{AB}\rangle_1\\ \langle v_{BC}\rangle_1\\ \langle v_{CA}\rangle_1\end{bmatrix}=-\dfrac{1}{RC}\begin{bmatrix}\langle v_{AB}\rangle_1\\ \langle v_{BC}\rangle_1\\ \langle v_{CA}\rangle_1\end{bmatrix}+\dfrac{1}{C}\begin{bmatrix}\langle i_{ab}\rangle_1\\ \langle i_{bc}\rangle_1\\ \langle i_{ca}\rangle_1\end{bmatrix}-j\begin{bmatrix}\langle v_{AB}\rangle_1\\ \langle v_{BC}\rangle_1\\ \langle v_{CA}\rangle_1\end{bmatrix}\\ \dfrac{d}{dt}\begin{bmatrix}\langle i_{ab}\rangle_0\\ \langle i_{bc}\rangle_0\\ \langle i_{ca}\rangle_0\end{bmatrix}=-\dfrac{r_L}{L}\begin{bmatrix}\langle i_{ab}\rangle_0\\ \langle i_{bc}\rangle_0\\ \langle i_{ca}\rangle_0\end{bmatrix}-\dfrac{1}{3L}\begin{bmatrix}\langle v_{AB}\rangle_0\\ \langle v_{BC}\rangle_0\\ \langle v_{CA}\rangle_0\end{bmatrix}+\dfrac{\sqrt{3}m}{6L}\begin{bmatrix}\left\langle v_{dc}\cos(\omega t-\varphi_a+\dfrac{\pi}{6})\right\rangle_0\\ \left\langle v_{dc}\cos(\omega t-\varphi_b+\dfrac{\pi}{6})\right\rangle_0\\ \left\langle v_{dc}\cos(\omega t-\varphi_c+\dfrac{\pi}{6})\right\rangle_0\end{bmatrix}\\ \dfrac{d}{dt}\begin{bmatrix}\langle v_{AB}\rangle_0\\ \langle v_{BC}\rangle_0\\ \langle v_{CA}\rangle_0\end{bmatrix}=-\dfrac{1}{RC}\begin{bmatrix}\langle v_{AB}\rangle_0\\ \langle v_{BC}\rangle_0\\ \langle v_{CA}\rangle_0\end{bmatrix}+\dfrac{1}{C}\begin{bmatrix}\langle i_{ab}\rangle_0\\ \langle i_{bc}\rangle_0\\ \langle i_{ca}\rangle_0\end{bmatrix}\end{cases} \tag{16}$$

The input DC voltage can be considered as a constant V_{dc}, thus it has

$$\langle v_{dc}\rangle_{\pm1}=0\ ,\ \langle v_{dc}\rangle_0=V_{dc} \tag{17}$$

According to equation (3) and (5), the following equations are not difficult to be acquired

$$\begin{aligned}&\left\langle v_{dc}\cos(\omega t-\varphi_k+\frac{\pi}{6})\right\rangle_1=\langle v_{dc}\rangle_1\left\langle\cos(\omega t-\varphi_k+\frac{\pi}{6})\right\rangle_0\\ &+\langle v_{dc}\rangle_0\left\langle\cos(\omega t-\varphi_k+\frac{\pi}{6})\right\rangle_1=\langle v_{dc}\rangle_0\left\langle\cos(\omega t-\varphi_k+\frac{\pi}{6})\right\rangle_1=\frac{1}{2}V_{dc}e^{-j(\varphi_k-\frac{\pi}{6})}\end{aligned} \tag{18}$$

$$\begin{aligned}&\left\langle v_{dc}\cos(\omega t-\varphi_k+\frac{\pi}{6})\right\rangle_0=\langle v_{dc}\rangle_1\left\langle\cos(\omega t-\varphi_k+\frac{\pi}{6})\right\rangle_{-1}+\langle v_{dc}\rangle_0\left\langle\cos(\omega t-\varphi_k+\frac{\pi}{6})\right\rangle_0\\ &+\langle v_{dc}\rangle_{-1}\left\langle\cos(\omega t-\varphi_k+\frac{\pi}{6})\right\rangle_1=\langle v_{dc}\rangle_0\left\langle\cos(\omega t-\varphi_k+\frac{\pi}{6})\right\rangle_0=0\end{aligned} \tag{19}$$

Assuming that

$$\begin{cases} \langle i_{ab} \rangle_1 = x_1 + jx_2 & \langle i_{bc} \rangle_1 = x_3 + jx_4 & \langle i_{ca} \rangle_1 = x_5 + jx_6 \\ \langle v_{AB} \rangle_1 = x_7 + jx_8 & \langle v_{BC} \rangle_1 = x_9 + jx_{10} & \langle v_{CA} \rangle_1 = x_{11} + jx_{12} \\ \langle i_{ab} \rangle_0 = x_{13} & \langle i_{bc} \rangle_0 = x_{14} & \langle i_{ca} \rangle_0 = x_{15} \\ \langle v_{AB} \rangle_0 = x_{16} & \langle v_{BC} \rangle_0 = x_{17} & \langle v_{CA} \rangle_0 = x_{18} \end{cases} \tag{20}$$

Combining equations (15) and (20), the result is written as

$$\begin{cases} i_{ab} \approx 2x_1 \cos \omega t + x_{13} - 2x_2 \sin \omega t \\ i_{bc} \approx 2x_3 \cos \omega t + x_{14} - 2x_4 \sin \omega t \\ i_{ca} \approx 2x_5 \cos \omega t + x_{15} - 2x_6 \sin \omega t \\ v_{AB} \approx 2x_7 \cos \omega t + x_{16} - 2x_8 \sin \omega t \\ v_{BC} \approx 2x_9 \cos \omega t + x_{17} - 2x_{10} \sin \omega t \\ v_{CA} \approx 2x_{11} \cos \omega t + x_{18} - 2x_{12} \sin \omega t \end{cases} \tag{21}$$

Considering the above six equations, the final generalized state space averaging model of three-phase three-wire inverter is determined by

$$\begin{bmatrix} \dot{x}_1 \\ \dot{x}_2 \\ \dot{x}_3 \\ \dot{x}_4 \\ \dot{x}_5 \\ \dot{x}_6 \\ \dot{x}_7 \\ \dot{x}_8 \\ \dot{x}_9 \\ \dot{x}_{10} \\ \dot{x}_{11} \\ \dot{x}_{12} \end{bmatrix} = \begin{bmatrix} -\frac{r_L}{L} & \omega & 0 & 0 & 0 & 0 & -\frac{1}{3L} & 0 & 0 & 0 & 0 & 0 \\ -\omega & -\frac{r_L}{L} & 0 & 0 & 0 & 0 & 0 & -\frac{1}{3L} & 0 & 0 & 0 & 0 \\ 0 & 0 & -\frac{r_L}{L} & \omega & 0 & 0 & 0 & 0 & -\frac{1}{3L} & 0 & 0 & 0 \\ 0 & 0 & -\omega & -\frac{r_L}{L} & 0 & 0 & 0 & 0 & 0 & -\frac{1}{3L} & 0 & 0 \\ 0 & 0 & 0 & 0 & -\frac{r_L}{L} & \omega & 0 & 0 & 0 & 0 & -\frac{1}{3L} & 0 \\ 0 & 0 & 0 & 0 & -\omega & -\frac{r_L}{L} & 0 & 0 & 0 & 0 & 0 & -\frac{1}{3L} \\ \frac{1}{C} & 0 & 0 & 0 & 0 & 0 & -\frac{1}{RC} & \omega & 0 & 0 & 0 & 0 \\ 0 & \frac{1}{C} & 0 & 0 & 0 & 0 & -\omega & -\frac{1}{RC} & 0 & 0 & 0 & 0 \\ 0 & 0 & \frac{1}{C} & 0 & 0 & 0 & 0 & 0 & -\frac{1}{RC} & \omega & 0 & 0 \\ 0 & 0 & 0 & \frac{1}{C} & 0 & 0 & 0 & 0 & -\omega & -\frac{1}{RC} & 0 & 0 \\ 0 & 0 & 0 & 0 & \frac{1}{C} & 0 & 0 & 0 & 0 & 0 & -\frac{1}{RC} & \omega \\ 0 & 0 & 0 & 0 & 0 & \frac{1}{C} & 0 & 0 & 0 & 0 & -\omega & -\frac{1}{RC} \end{bmatrix} \begin{bmatrix} x_1 \\ x_2 \\ x_3 \\ x_4 \\ x_5 \\ x_6 \\ x_7 \\ x_8 \\ x_9 \\ x_{10} \\ x_{11} \\ x_{12} \end{bmatrix} + \begin{bmatrix} \frac{\sqrt{3}mV_{dc}\cos(\varphi_a - \frac{\pi}{6})}{12L} \\ -\frac{\sqrt{3}mV_{dc}\sin(\varphi_a - \frac{\pi}{6})}{12L} \\ \frac{\sqrt{3}mV_{dc}\cos(\varphi_b - \frac{\pi}{6})}{12L} \\ -\frac{\sqrt{3}mV_{dc}\sin(\varphi_b - \frac{\pi}{6})}{12L} \\ \frac{\sqrt{3}mV_{dc}\cos(\varphi_c - \frac{\pi}{6})}{12L} \\ -\frac{\sqrt{3}mV_{dc}\sin(\varphi_c - \frac{\pi}{6})}{12L} \\ 0 \\ 0 \\ 0 \\ 0 \\ 0 \\ 0 \end{bmatrix} \tag{22}$$

$$\begin{bmatrix} \dot{x}_{13} \\ \dot{x}_{14} \\ \dot{x}_{15} \\ \dot{x}_{16} \\ \dot{x}_{17} \\ \dot{x}_{18} \end{bmatrix} = \begin{bmatrix} -\frac{r_L}{L} & 0 & 0 & -\frac{1}{3L} & 0 & 0 \\ 0 & -\frac{r_L}{L} & 0 & 0 & -\frac{1}{3L} & 0 \\ 0 & 0 & -\frac{r_L}{L} & 0 & 0 & -\frac{1}{3L} \\ \frac{1}{C} & 0 & 0 & -\frac{1}{RC} & 0 & 0 \\ 0 & \frac{1}{C} & 0 & 0 & -\frac{1}{RC} & 0 \\ 0 & 0 & \frac{1}{C} & 0 & 0 & -\frac{1}{RC} \end{bmatrix} \begin{bmatrix} x_{13} \\ x_{14} \\ x_{15} \\ x_{16} \\ x_{17} \\ x_{18} \end{bmatrix} \tag{23}$$

In order to prevent the two IGBTs in the same leg from shoot-through current, the dead time is indispensable. However, the dead time will reduce the output voltage and current fundamental amplitude.

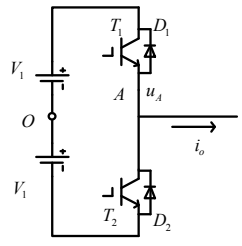

Fig. 2. Phase leg of three-phase inverter

For the sake of analytical simplification, a phase leg of three-phase leg is shown in the Fig.2, where $V_{dc}=2V_1$.

Fig.3 dipicts us the dead time effect of the output voltage in a fundamental period. Fig.3 (a) represents the ideal output waveform and its fundamental component, Fig.3 (b) shows us the waveform of the output current, where, φ is the power factor angle, the influences on output voltage caused by dead time can be seen in Fig.3(c), where, v_d is the error of output voltage, v_{do} is its fundamental component.

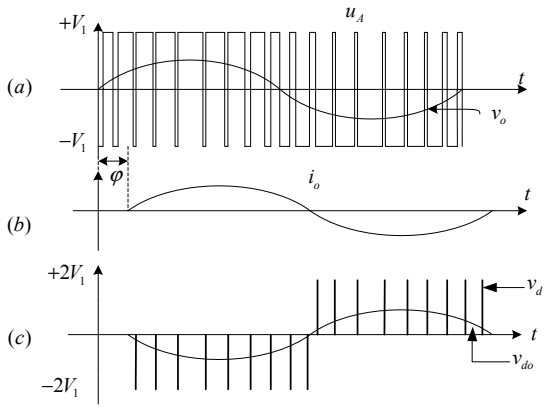

Fig. 3. The dead time effect in a fundamental period

From the above figure, we can easily learn that the voltage error is composed of pulse sequence, whose pulse width is dead time t_d. The pulse sequence in a fundamental period can be equivalent to a square wave, whose amplitude is calculated by

$$U_d = N \bullet t_d \bullet 2V_1 \bullet \frac{1}{T} = \frac{f_c}{f} \bullet t_d \bullet 2V_1 \bullet f = f_c \bullet t_d \bullet 2V_1 \tag{24}$$

where, f_c is switching frequency, T and f are fundamental period and frequency separately, t_d is dead time, $2V_1$ is input voltage.

In the three-phase half bridge inverter system, the fundamental component of the output voltage can be expressed by

$$v_o(t) = mV_1 \sin \omega t \tag{25}$$

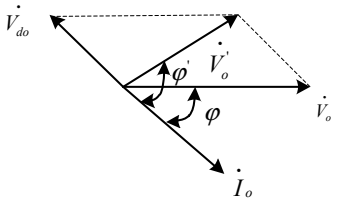

Fig. 4. The vectors diagram of dead time effect

As is shown in Fig.4, v_o' represents the actual output fundamental voltage. According to cosine theorem, v_o' can be expressed by

$$v_o'^2 = v_o^2 + v_{do}^2 - 2v_o v_{do} \cos \varphi \tag{26}$$

Then the following equation is obtained

$$\frac{v_o'}{v_o} = \sqrt{1 + (\frac{v_{do}}{v_o})^2 - 2\frac{v_{do}}{v_o}\cos\varphi} = \sqrt{1 + (K)^2 - 2K\cos\varphi} \tag{27}$$

where, K is calculated by

$$K=\frac{4U_d}{\sqrt{2}\pi}\Big/\frac{mV_1}{\sqrt{2}}=\frac{4U_d}{mV_1}=\frac{8f_ct_d}{m\pi} \tag{28}$$

Because of the symmetry of each phase, the fundamental amplitude of actual output line voltage v'_{AB} and the ideal one v_{AB} also satisfy the following ratio

$$\frac{v'_{AB}}{v_{AB}}=\sqrt{1+K^2-2K\cos\varphi} \tag{29}$$

Due to the constancy of load, the above equation is likewise suitable for the fundamental amplitude of virtual line current i'_{ab} and the ideal one i_{ab}

$$\frac{i'_{ab}}{i_{ab}}=\sqrt{1+K^2-2K\cos\varphi} \tag{30}$$

Only resistive load is considered in the modeling, therefore, $\varphi=0$. Consequently, the above two equations is simplified by

$$\frac{v'_{AB}}{v_{AB}}=\frac{i'_{ab}}{i_{ab}}=1-K \tag{31}$$

Actually, thanks to the control of DC suppression, the DC components of output voltages had been eliminated. The equations about DC components in equation (16) can be ignored.

Based on the above equations, the equation (16) is modified by

$$\begin{cases}\dfrac{d}{dt}\begin{bmatrix}\langle i'_{ab}\rangle_1\\ \langle i'_{bc}\rangle_1\\ \langle i'_{ca}\rangle_1\end{bmatrix}=-\dfrac{r_L}{L}\begin{bmatrix}\langle i'_{ab}\rangle_1\\ \langle i'_{bc}\rangle_1\\ \langle i'_{ca}\rangle_1\end{bmatrix}-\dfrac{1}{3L}\begin{bmatrix}\langle v'_{AB}\rangle_1\\ \langle v'_{BC}\rangle_1\\ \langle v'_{CA}\rangle_1\end{bmatrix}+\dfrac{\sqrt{3}m(1-K)}{6L}\begin{bmatrix}\left\langle v_{dc}\cos(\omega t-\varphi_a+\frac{\pi}{6})\right\rangle_1\\ \left\langle v_{dc}\cos(\omega t-\varphi_b+\frac{\pi}{6})\right\rangle_1\\ \left\langle v_{dc}\cos(\omega t-\varphi_c+\frac{\pi}{6})\right\rangle_1\end{bmatrix}-j\omega\begin{bmatrix}\langle i'_{ab}\rangle_1\\ \langle i'_{bc}\rangle_1\\ \langle i'_{ca}\rangle_1\end{bmatrix}\\ \dfrac{d}{dt}\begin{bmatrix}\langle v'_{AB}\rangle_1\\ \langle v'_{BC}\rangle_1\\ \langle v'_{CA}\rangle_1\end{bmatrix}=-\dfrac{1}{RC}\begin{bmatrix}\langle v'_{AB}\rangle_1\\ \langle v'_{BC}\rangle_1\\ \langle v'_{CA}\rangle_1\end{bmatrix}+\dfrac{1}{C}\begin{bmatrix}\langle i'_{ab}\rangle_1\\ \langle i'_{bc}\rangle_1\\ \langle i'_{ca}\rangle_1\end{bmatrix}-j\begin{bmatrix}\langle v'_{AB}\rangle_1\\ \langle v'_{BC}\rangle_1\\ \langle v'_{CA}\rangle_1\end{bmatrix}\end{cases} \tag{32}$$

Assuming that

$$\begin{cases}\langle i'_{ab}\rangle_1=x'_1+jx'_2 & \langle i'_{bc}\rangle_1=x'_3+jx'_4 & \langle i'_{bc}\rangle_1=x'_3+jx'_4\\ \langle v'_{AB}\rangle_1=x'_7+jx'_8 & \langle v'_{BC}\rangle_1=x'_9+jx'_{10} & \langle v'_{CA}\rangle_1=x'_{11}+jx'_{12}\end{cases} \tag{33}$$

Likewise, the modified generalized state space averaging model of three-phase three-wire inverter which takes dead-time effect into account can be expressed by

$$\begin{bmatrix}\dot{x}'_1\\ \dot{x}'_2\\ \dot{x}'_3\\ \dot{x}'_4\\ \dot{x}'_5\\ \dot{x}'_6\\ \dot{x}'_7\\ \dot{x}'_8\\ \dot{x}'_9\\ \dot{x}'_{10}\\ \dot{x}'_{11}\\ \dot{x}'_{12}\end{bmatrix}=\begin{bmatrix}-\frac{r_L}{L} & \omega & 0 & 0 & 0 & 0 & -\frac{1}{3L} & 0 & 0 & 0 & 0 & 0\\ -\omega & -\frac{r_L}{L} & 0 & 0 & 0 & 0 & 0 & -\frac{1}{3L} & 0 & 0 & 0 & 0\\ 0 & 0 & -\frac{r_L}{L} & \omega & 0 & 0 & 0 & 0 & -\frac{1}{3L} & 0 & 0 & 0\\ 0 & 0 & -\omega & -\frac{r_L}{L} & 0 & 0 & 0 & 0 & 0 & -\frac{1}{3L} & 0 & 0\\ 0 & 0 & 0 & 0 & -\frac{r_L}{L} & \omega & 0 & 0 & 0 & 0 & -\frac{1}{3L} & 0\\ 0 & 0 & 0 & 0 & -\omega & -\frac{r_L}{L} & 0 & 0 & 0 & 0 & 0 & -\frac{1}{3L}\\ \frac{1}{C} & 0 & 0 & 0 & 0 & 0 & -\frac{1}{RC} & \omega & 0 & 0 & 0 & 0\\ 0 & \frac{1}{C} & 0 & 0 & 0 & 0 & -\omega & -\frac{1}{RC} & 0 & 0 & 0 & 0\\ 0 & 0 & \frac{1}{C} & 0 & 0 & 0 & 0 & 0 & -\frac{1}{RC} & \omega & 0 & 0\\ 0 & 0 & 0 & \frac{1}{C} & 0 & 0 & 0 & 0 & -\omega & -\frac{1}{RC} & 0 & 0\\ 0 & 0 & 0 & 0 & \frac{1}{C} & 0 & 0 & 0 & 0 & 0 & -\frac{1}{RC} & \omega\\ 0 & 0 & 0 & 0 & 0 & \frac{1}{C} & 0 & 0 & 0 & 0 & -\omega & -\frac{1}{RC}\end{bmatrix}\begin{bmatrix}x'_1\\ x'_2\\ x'_3\\ x'_4\\ x'_5\\ x'_6\\ x'_7\\ x'_8\\ x'_9\\ x'_{10}\\ x'_{11}\\ x'_{12}\end{bmatrix}+\begin{bmatrix}\frac{\sqrt{3}mV_{dc}(1-K)\cos(\varphi_a-\frac{\pi}{6})}{12L}\\ -\frac{\sqrt{3}mV_{dc}(1-K)\sin(\varphi_a-\frac{\pi}{6})}{12L}\\ \frac{\sqrt{3}mV_{dc}(1-K)\cos(\varphi_b-\frac{\pi}{6})}{12L}\\ -\frac{\sqrt{3}mV_{dc}(1-K)\sin(\varphi_b-\frac{\pi}{6})}{12L}\\ \frac{\sqrt{3}mV_{dc}(1-K)\cos(\varphi_c-\frac{\pi}{6})}{12L}\\ -\frac{\sqrt{3}mV_{dc}(1-K)\sin(\varphi_c-\frac{\pi}{6})}{12L}\\ 0\\ 0\\ 0\\ 0\\ 0\\ 0\end{bmatrix} \tag{34}$$

where amplitude modulation ratio m, initial phase angle φ_0, dead time t_d and switching frequency f_c are control parameters.

IV. SIMULATION AND EXPERIMENTAL VERIFICATION

In order to validate the accuracy of modeling of three-phase inverter based on the generalized state space averaging method, the simulation was carried out by Matlab, and the experiment was proceed in a 3kW three-phase three-wire inverter. The corresponding parameters are listed in Table I.

TABLE I PARAMETERS OF SIMULATION AND EXPERIMENT

Symbol	Description	Value	Unit
V_{dc}	*Input voltage*	200	V
m	*Amplitude modulation ratio*	0.9	-
f	*Fundamental frequency*	50	Hz
f_c	*Switching frequency*	20	kHz
t_d	*Dead time*	2.0	μs
φ_0	*Initial phase angle*	0	rad/s
L	*Filtering inductor*	3.4	mH
r_L	*ESR of filtering inductor*	0.2	Ω
C	*Filter capacitor*	2.2	μF
R	*Loads resistor*	140	Ω

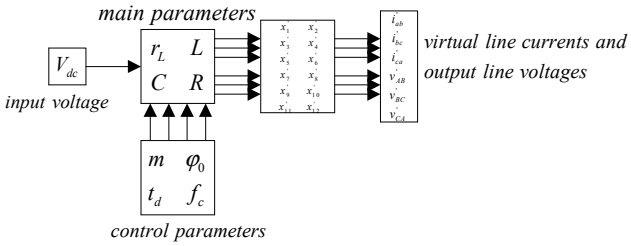

Fig. 5. Control block diagram of simulation model based on generalize averaging method

The control block diagram of simulation model based on generalized averaging method is shown in Fig. 5.

As is illustrated in Fig.5, m, φ_0, t_d and f_c are control parameters, r_L, L, C and R are main parameters, whose values are given in Table I. Finally, we acquire the waveforms of virtual line currents and output line voltages, which are composed of state variables.

Analogously, the control block diagram of simulation model and experiment of actual devices is shown in Fig. 6.

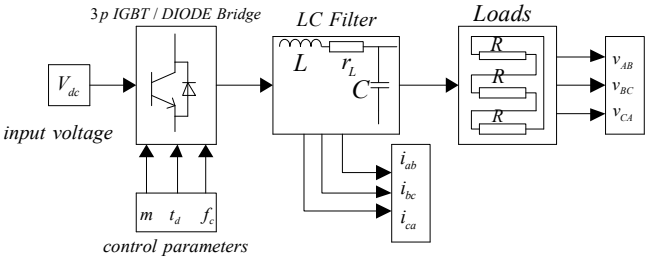

Fig. 6. Control block diagram of simulation model of actual devices

In Fig.6, 3p Invert Bridge consists of six IGBTs with an antiparallel diode separately. In addition, m, t_d, f_c are control parameters. Three-phase symmetrical resistors in delta connection make up of the loads.

In order to validate the precision of generalized averaging method more efficaciously, simulation model based on generalized averaging method, simulation model of actual devices and experiment were proceeded with various dead

time t_d, amplitude modulation ratio m and switching frequency f_c. With the same simulation parameters, required simulation time of switching model is almost twice as long as that of generalized averaging model.

According to the data of simulation and experiments, the peak-to-peak values of fundamental components of output line voltages and virtual line currents are listed in the following tables.

TABLE II PEAK-TO-PEAK VALUE ($f_c = 20kHz$, $m = 0.9$)

$t_d/\mu s$		2	2.2	2.4	2.6	2.8	3
Generalized averaging method	i_{ab}/A	1.979	1.954	1.929	1.903	1.878	1.853
	v_{AB}/V	275.8	272.2	268.8	265.1	261.7	258.3
Simulation of actual device	i_{ab}/A	1.975	1.956	1.933	1.907	1.87	1.851
	v_{AB}/V	275.4	272.6	269.5	265.7	260.6	257.9
Experiment results	i_{ab}/A	1.947	1.92	1.907	1.88	1.853	1.84
	v_{AB}/V	272	268	265	262	258	255
Generalized method vs switch model	$i_{ab}/\%$	0.20	0.1	0.21	0.21	0.43	0.11
	$v_{AB}/\%$	0.14	0.15	0.26	0.22	0.42	0.16
Generalized method vs experiment	$i_{ab}/\%$	1.6	1.8	1.2	1.2	1.3	0.71
	$v_{AB}/\%$	1.4	1.6	1.4	1.2	1.4	1.3

TABLE III PEAK-TO-PEAK VALUES ($t_d = 2\mu s$, $m = 0.9$)

f_c/kHz		5	10	15	20	25	30
Generalized averaging method	i_{ab}/A	2.17	2.105	2.042	1.979	1.916	1.853
	v_{AB}/V	302.3	293.3	284.6	275.8	267	258.3
Simulation of actual device	i_{ab}/A	2.173	2.11	2.046	1.975	1.902	1.856
	v_{AB}/V	302.5	294.1	285.1	275.4	264	258.7
Experiment results	i_{ab}/A	2.153	2.107	2.023	1.957	1.907	1.84
	v_{AB}/V	300	292	283	272	263	254
Generalized method vs switch model	$i_{ab}/\%$	0.14	0.24	0.20	0.20	0.74	0.16
	$v_{AB}/\%$	0.07	0.27	0.18	0.14	1.1	0.15
Generalized method vs experiment	$i_{ab}/\%$	0.79	0.24	0.94	1.1	0.47	0.71
	$v_{AB}/\%$	0.77	0.44	0.56	1.4	1.5	1.7

TABLE IV PEAK-TO-PEAK VALUES ($f_c = 20kHz$, $t_d = 2\mu s$)

m		0.4	0.5	0.6	0.7	0.8	0.9
Generalized averaging method	i_{ab}/A	0.739	0.987	1.229	1.483	1.731	1.979
	v_{AB}/V	103	137.6	171.1	206.7	241.3	275.8
Simulation of actual device	i_{ab}/A	0.754	0.983	1.214	1.497	1.741	1.975
	v_{AB}/V	105	137	168.7	208.8	242.7	275.4
Experiment results	i_{ab}/A	0.75	0.97	1.206	1.48	1.72	1.947
	v_{AB}/V	102	135	168	206	242	272
Generalized method vs switch model	$i_{ab}/\%$	2.0	0.41	1.2	0.94	0.57	0.20
	$v_{AB}/\%$	1.9	1.8	2.0	1.0	0.58	0.14
Generalized method vs experiment	$i_{ab}/\%$	1.5	0.44	1.4	0.20	0.64	1.6
	$v_{AB}/\%$	0.98	0.92	1.8	0.34	0.29	1.4

The data in the tables have shown us that with the same circuit parameters, generalized averaging model coincides with the simulation and experiment of actual devices commendably, with desired relative errors within 2%. In addition, Table II and Table III show us the fundamental components of virtual line currents and output line voltages almost decrease linearly with the increase of dead time and switch frequency. In contrast, it is easily learned from Table IV that with the enhancement of amplitude modulation ratio, the fundamental components of virtual line currents and output line voltages nearly increase linearly.

TABLE V PARAMETERS OF EXPERIMENT

Symbol	Description	Value	Unit
V_{dc}	*Input voltage*	250	V
V_{ref}	*Amplitude of reference voltage*	150	V
f	*Fundamental frequency*	50	Hz
f_c	*Switching frequency*	20	kHz
t_d	*Dead time*	2.0	μs
L	*Filtering inductor*	3.4	mH
r_L	*ESR of filtering inductor*	0.2	Ω
C	*Filter capacitor*	2.2	μF
R	*Loads resistor*	70/140	Ω
C_{non}	*Capacitor of nonlinear loads*	2200	μF
R_{non}	*Resistor of nonlinear loads*	160	Ω
K_{vp}	*Proportion parameter of voltage loop*	0.01	-
K_{vi}	*Integration parameter of voltage loop*	54	-
K_{ip}	*Proportion parameter of current loop*	0.2	-
K_{ii}	*Integration parameter of current loop*	10	-

Based on the proposed generalized averaging method, PI controllers including outer loop of voltage and inner loop of current are designed accordingly. The corresponding parameters are illustrated in Table V.

The following experimental waveforms are obtained on the basis of the above parameters.

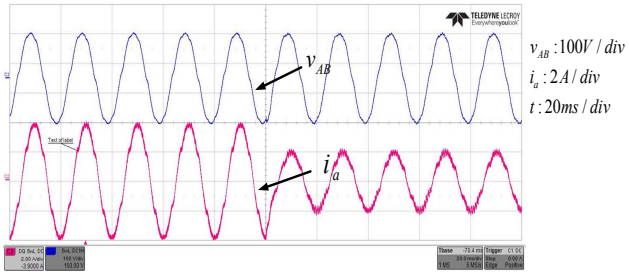

Fig. 7. The transient process of output line voltage and inductor current from full loads(70Ω) to half loads(140Ω)

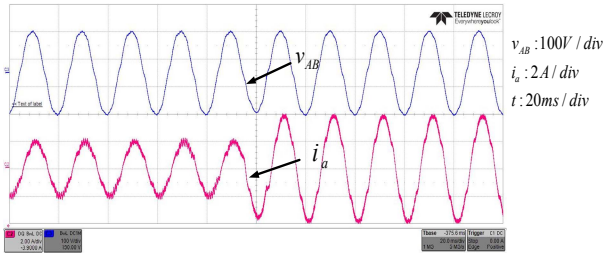

Fig. 8. The transient process of output line voltage and inductor current from half loads(140Ω) to full loads(70Ω)

As is shown in Fig.7 and Fig.8, the closeloop controlled parameters calculated by the proposed model provides

powerful means for fast and precise steady-state and transient analysis.The calculated control parameters are in accordance with the actual control parameters commendably.

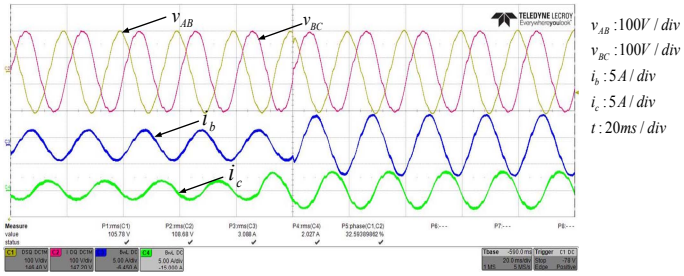

Fig. 9. The transient process of output line voltages and inductor currents from half loads(*70Ω,140Ω,140Ω*) to full loads(*35Ω,70Ω,70Ω*)

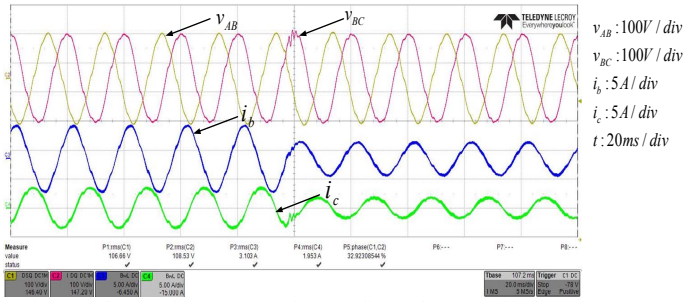

Fig. 10. The transient process of output line voltages and inductor currents from half loads(*35Ω,70Ω,70Ω*) to full loads(*70Ω,140Ω,140Ω*)

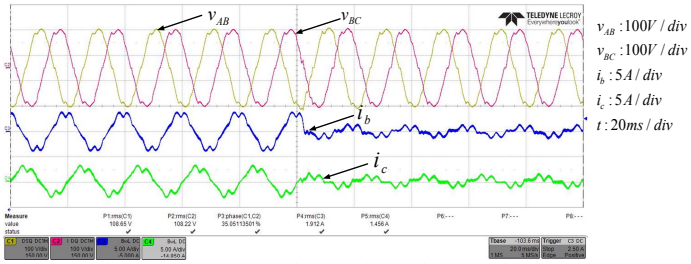

Fig. 11. The transient process of output line voltages and inductor currents from mixed loads to nonlinear loads

In order to further prove the accuracy and validity of PI controllers based on the proposed generalized averaging method , added experiments were proceeded with other types of loads, which are illustrated in Fig.9, Fig.10 and Fig.11. Besides, nonlinear loads in Fig.11 is composed of three-phase rectifier bridge in parallel with a capacitor and a resistor, whose values are *2200μF* and *160Ω* respectively. Moreover, mixed loads consist nonlinear loads in parallel with unbalanced loads (*70Ω*, *140Ω*, *140Ω*).

V. CONCLUSION

In this paper, the modeling of three-phase three-wire inverter based on generalized averaging method , which takes dead-time effect into consideration , is illustrated in detail. The simulation and experiment of actual inverter validate the correctness and efficiency of the proposed model, regarding the influence of different parameters such as amplitude modulation ratio, dead time and switching frequency. The proposed model can greatly guarantee the accuracy of fundamental components of voltages and currents and improve the calculation efficiency in simulation of inverters. Besides, the proposed method is further used in the closeloop controller design for the single inverter. The experimental waveforms demonstrate the veracity of the proposed model all the more. It is conceivable that the proposed method can be ulteriorly utilized in the controller design of parallel connection of several inverters or circumfluence calculation and elimination among different inverters.

ACKNOWLEDGEMENT

This project is supported by National Natural Science Foundation of China (51177149), and Zhejiang Key Science and Technology Innovation Group Program (2010R50021).

REFERENCES

[1] Byoung-Kuk Lee, Mehrdad Ehsani, "A Simplified Functional Simulation Model for Three-Phase Voltage-Source Inverter Using Switching Function Concept," *IEEE Transactions on Industrial Electronics*, vol.48, no.2, pp. 309-321, April 2001.

[2] Xupeng Fang, "Modeling of Voltage-fed Z-source Inverter by Switching Functions," *IEEE International Conference on Industrial Technology*, pp. 1-6, April 2008.

[3] Runxin Wang, Jinjun Liu, "Redefining a New-Formed Average Model for Three-Phase Boost Rectifiers/Voltage Source Inverters," *The 24th Applied Power Electronics Conference and Exposition*, pp. 1680-1686, February 2009.

[4] M. Davari, A. R. Pourshoghi, I.Salabeigi, G. B.Gharehpetian and S.H.Fathi, "A New Nonlinear Controller Design Using Average State Space Model of the Inverter-Based Distributed Generation to Mitigate Power Quality Problems," *International Conference on Electronic Machines and Systems*, pp. 1-5, November 2009.

[5] N. Kroutikova, C.A.Hernandez-Aramburo and T.C. Green, "State-space model of grid-connected inverters under current control mode," *The Institution of Engineering and Technology*, 2007, vol.1, no.3, pp. 329-338.

[6] Seth R. Sanders, J. Mark Noworolski, Xiaojun Z. Liu, and George C. Verghese, "Generalized averaging method for power conversion circuits," *IEEE Transactions on Power Electronics*, vol.6, no.2, pp. 251-259, April 1991.

[7] Toni Itkonen, Julius Luukko, "Switching-Function-Based Simulation Model for Three-Phase Voltage Source Inverter Taking Dead-Time Effects into Account," *The 34th IEEE Annual Conference on Industrial Electronics*, pp. 992-997, November 2008.

[8] S. Ahmed, Z. Shen, P. Mattavelli, D. Boroyevich, M. Jaksic, K. Kamiar and J. Fu, "Small-Signal Model of a Voltage Source Inverter(VSI) Considering the Dead-Time Effect and Space Vector Modulation Types," *The 26th Applied Power Electronics Conference and Exposition*, pp. 685-690, March 2011.